Journal of Colloid and Interface Science **209,** 72–78 (1999)
Article ID jcis.1998.5893, available online at http://www.idealibrary.com on IDEAL®

Role of Surface Precipitation in Copper Sorption by the Hydrous Oxides of Iron and Aluminum

K. G. Karthikeyan,* Herschel A. Elliott,*,[1] and Jon Chorover†

Agricultural and Biological Engineering Department and †Agronomy Department, The Pennsylvania State University, University Park, Pennsylvania 16802

Received April 22, 1998; accepted September 30, 1998

Isotherms were developed at pH 6.9 for adsorption (ADS) and coprecipitation (CPT) of Cu by hydrous oxides of Fe (HFO) and Al (HAO) to study the role of sorbate/sorbent ratio in metal cation removal. For low sorbate/sorbent conditions, HFO had a higher Cu retention capacity than HAO regardless of contact methodology. For either oxide, CPT was consistently more effective than ADS in removing Cu from solution. At high sorbate/sorbent ratios, surface precipitation dominates and the oxide's net cation retention capacity depends on the nature and solubility of the precipitate formed at the oxide–water interface. X-ray diffraction patterns and isotherms of HAO for both ADS and CPT suggest formation of a solid solution [e.g., $CuAl_2O_4$(s)] with dramatically lower solubility than $Cu(OH)_2$(s) precipitated in bulk solution. In contrast, Cu precipitated on the HFO surface exhibited a solubility comparable to the bulk precipitated $Cu(OH)_2$(s). Therefore, at high sorbate/sorbent ratios, HAO has a higher Cu "apparent" sorption capacity than HFO. The relative utility of these oxides as metal scavengers thus depends markedly on sorbate/sorbent conditions.

Key Words: **surface precipitation; sorption; isotherms; X-ray diffraction; hydrous iron oxide; hydrous aluminum oxide; copper.**

INTRODUCTION

Hydrous oxides of iron (HFO) and aluminum (HAO) are important mineral components of natural systems. These oxides have a high capacity to sorb heavy metals and thus play a significant role in controlling their availability and mobility in the environment. As strong sorbents, these oxides can also be employed to treat industrial and municipal wastewaters containing heavy metals.

Depending on the relative concentrations and contact methods, interactions between hydrous oxides and metals, can include: (a) *adsorption*, a surface complexation reaction between surface sites and metal sorbates; (b) *surface precipitation*, formation of a multilayer solid phase on the oxide surface (1); and (c) *coprecipitation*, the simultaneous precipitation of the sorbate ion with the hydrous oxide phase. These processes can act simultaneously and distinguishing them is difficult and requires analytical methods with molecular-scale resolution (2). Depending on the type of interaction, metals exhibit different solubilities that can dramatically alter environmental mobility and removal efficiency during wastewater treatment.

Numerous studies of metal sorption by hydrous oxides are available (3–14), with relatively few considering coprecipitation as a potential mechanism (4, 5, 10–13). In an earlier publication, we compared adsorption and coprecipitation of Cu with HFO and HAO as a function of pH (15). While most prior investigations have focused on very low sorbate-to-sorbent (e.g., Cu/Fe) ratios (<0.01), a wider range is required to study the transition between adsorption and surface precipitation. Recently, Katz and Hayes (16, 17) used surface polymerization reactions to model the transition between adsorption and precipitation. The primary objective of this study was, therefore, to investigate the interaction of Cu with HFO and HAO, focusing on the effect of sorbate-to-sorbent ratio and the onset of surface precipitation. X-ray diffraction was used to ascertain the nature of Cu interaction with the oxide surface.

MATERIALS AND METHODS

HFO and HAO were prepared from ferric chloride [$FeCl_3 \cdot 6H_2O$] and aluminum sulfate [alum, $Al_2(SO_4)_3 \cdot 16H_2O$], salts that are commonly used in water treatment. Although anion type (Cl^- vs SO_4^{2-}) may influence precipitate morphology (18–20), it does not significantly affect the amount of Cu sorbed under the conditions of this study (21). The surface areas of HFO and HAO were determined by BET-N_2 adsorption to be 187 and 99 m^2/g, respectively. Experiments were conducted at pH 6.9 ± 0.05 with Fe_T and Al_T concentrations of 10^{-3} M. Assuming negligible soluble Fe/Al, ionic strength for the HFO and HAO systems was 0.0135 and 0.0122 M, respectively. Prior to each experiment, fresh $FeCl_3$ and alum solutions were prepared and adjusted to pH < 2.2 and < 3.5, respectively, to prevent premature precipitate formation. The Cu stock solution was prepared from reagent-grade cupric chloride [$CuCl_2 \cdot 2H_2O$]. All solutions were made using distilled-deionized water and reaction beakers were soaked in 20% HNO_3 for 16 h prior to use. The pH adjustments were

[1] To whom correspondence should be addressed at The Pennsylvania State University, 208 Agricultural Sciences & Industries Building, University Park, PA 16802-3505.

0021-9797/99 $30.00

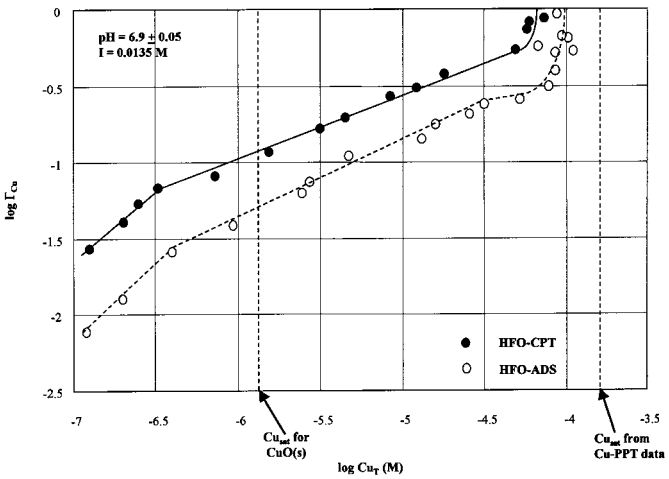

FIG. 1. Sorption isotherms for HFO–ADS and HFO–CPT. Cu_T is the total soluble concentration and Γ_{Cu} is the Cu sorption density (mol Cu sorbed/mol Fe added). HFO was obtained by the addition of 10^{-3}M as Fe^{3+} of $FeCl_3 \cdot 6H_2O$. $Cu_{sat} = 10^{-3.8}$M from the Cu-PPT data in Karthikeyan *et al.* (15).

made with 0.02–1 N KOH and all experiments were conducted at 18 ± 0.5°C.

Batch experiments were performed in 150-mL beakers with a reaction time of 45 min used to study the initial sorption process and mimic full-scale flocculation (3, 5). Solutions were mixed with a magnetic stirrer operated at 40 rpm. Gentle mixing conditions (velocity gradient = 5–10 s^{-1}) were employed to facilitate stable floc formation.

Adsorption experiments. For adsorption experiments (ADS), hydrous oxide colloids were preformed by gradually increasing the pH of a 100-mL solution of alum or $FeCl_3$. After aging the hydrous oxide suspensions for 10 min, 5 mL of Cu solution was added and the suspension was mixed.

Coprecipitation experiments. Coprecipitation experiments (CPT) involved the formation of hydrous oxide colloid in the presence of Cu. The alum or $FeCl_3$ and Cu solutions were initially combined, the pH was slowly increased to the target level, and the system was mixed. After equilibration, pH was measured and the suspension was allowed to settle for 20 min. The samples were then filtered through a 0.45-μm (Millipore) filter. The filtrate was acidified to pH < 2 and Cu was analyzed using flame atomic absorption spectrophotometry (Cu detection limit = 2 μg/L). To account for metal sorption onto the reaction vessels, blanks (no $FeCl_3$/alum addition) were run for all experiments. It is important to realize that the abbreviations ADS and CPT used herein refer to experimental protocol and not necessarily the nature of the sorbate/sorbent interactions.

X-ray diffraction. X-ray diffraction (XRD) analysis was conducted to characterize the oxides generated as above with Cu/Fe molar ratio of 0.18 and Cu/Al molar ratio of 0.21 [$Fe_T = 0.01875$ M; $Al_T = 0.0161$ M; $Cu_T = 0.003415$ M]. Samples were prepared under a variety of pH conditions to provide a range of surface Cu coverages. After reaction and settling, the solids were separated by centrifugation (2000 rpm for 20 min), freeze–dried for at least 16 h, and then subjected to XRD analysis. Unless otherwise noted, solid phases were identified using the standard "d" spacing for minerals given in powder diffraction files (22) or those found in the literature for similar compounds. All patterns were collected using a Phillips diffractometer (Mo$K\alpha$ radiation, maximum intensity = 300 counts).

RESULTS AND DISCUSSION

The effect of sorbate-to-sorbent ratio on adsorption and coprecipitation is illustrated using sorption isotherms (Figs. 1 and 2) wherein soluble Cu concentration (log Cu_T) is plotted against the sorption density (log Γ_{Cu}, where Γ_{Cu} is mol Cu sorbed/mol Fe or Al added). In a double logarithmic format, these isotherms typically have an initial region with unit slope at low Cu_T (called "linear," since a unit slope in log–log format results in a linear arithmetic plot), a Freundlich region with less than 1:1 slope, and a saturation region corresponding to full occupancy of sorbent reactive sites (6). As detailed below, the linear and Freundlich portions reflect removal of Cu by adsorption (i.e., surface complexation reactions). At higher Cu_T values, near the concentration sufficient for homogeneous precipitation of the sorbate, Γ_{Cu} increased sharply with Cu_T. This region corresponds to metal removal by precipitation reactions.

HFO–ADS

For the HFO–ADS system (Fig. 1), the concentration of sites with high binding strength (Type 1 sites) can be obtained from the Γ_{Cu} value at termination of the linear portion of the isotherm (23). From Fig. 1, the Type 1 site density was 0.028 mol

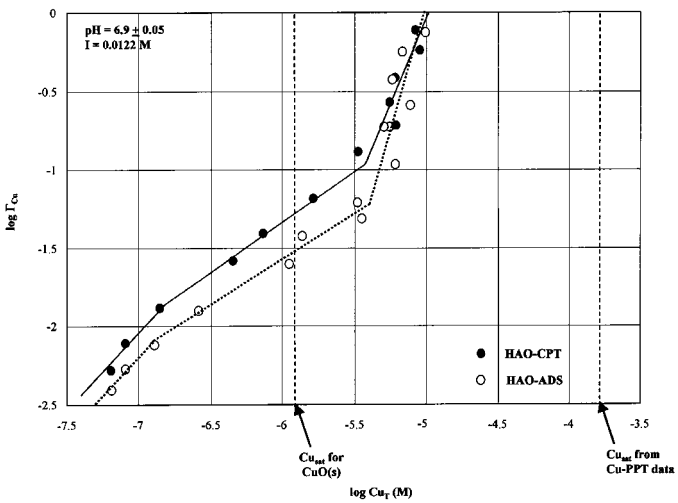

FIG. 2. Sorption isotherms for HAO–ADS and HAO–CPT. Cu_T is the total soluble concentration and Γ_{Cu} is the Cu sorption density (mol Cu sorbed/mol Al added). HAO was obtained by the addition of 10^{-3}M as Al^{3+} of $Al_2(SO_4)_3 \cdot 16H_2O$. $Cu_{sat} = 10^{-3.8}$M from the Cu-PPT data in Karthikeyan *et al.* (15).

Cu/mol Fe ($\log \Gamma_{Cu} = -1.56$), about an order of magnitude higher than values reported in Dzombak and Morel (23). The Type 2 site density (total reactive sites), which corresponds to the Γ_{Cu} at the saturation region, is 0.25 mol Cu/mol Fe ($\log \Gamma_{Cu} = -0.6$). This value is slightly higher than that of 0.2 reported in Dzombak and Morel (23). Estimates of site densities differ between studies because they are affected by pH and solids concentration (23). Isotherms reported by Dzombak and Morel (23) were obtained at pH < 5.5. The use of a higher pH (6.9) in this study could account for the higher Types 1 and 2 site densities measured.

The linear region for HFO–ADS extended to Cu_T of $10^{-6.4}$ M and the Freundlich region (slope of 0.7) to between Cu_T of $10^{-6.4}$ and $10^{-4.5}$ M. At Γ_{Cu} approaching site saturation values, the sorption isotherm should level off. However, as Cu_T increases above $10^{-4.2}$ M, there is an increase in Γ_{Cu}, presumably signaling the onset of surface precipitation of Cu. At high surface coverage, cation adsorption may lead to the formation of a surface precipitate (24). In theory, precipitative removal should exhibit a near-vertical isotherm (i.e., a stability boundary). However, laboratory isotherms exhibit a gradual (finite slope) increase in Γ_{Cu}, which, according to Farley *et al.* (7), indicates a continuum between surface reactions and precipitation. The solubility product of the surface precipitate (K_{spCu}) formed during HFO–ADS calculated to be $10^{9.46}$ is slightly lower than that of $10^{9.88}$ obtained for homogeneous Cu precipitation (Cu-PPT). K_{spCu} is defined as $\{Cu^{2+}\}/\{H^+\}^2$, where $\{Cu^{2+}\}$ was obtained from the mean Cu_T values ($10^{-4.11}$ M for HFO–ADS) corresponding to the best-fit of data in the surface precipitation region. We assumed that $[\{Cu_T\} = [\{Cu^{2+}\} + \{CuOH^+\} + \{Cu(OH)_2^0\} + \{Cu(OH)_3^-\} + \{Cu(OH)_4^{2-}\}]$. Equilibrium constants for the hydrolysis reactions of Cu^{2+} were obtained from Stumm and Morgan (24). For Cu-PPT, Cu_T of $10^{-3.8}$ M at pH 6.9 was obtained by the extrapolation of our Cu-PPT data (15). Therefore, the surface precipitate formed on HFO had a slightly lower solubility compared to that seen with homogeneous $Cu(OH)_2$(s) under similar experimental conditions. The shape of our HFO–ADS isotherm conforms to that developed by Van Cappellen (25) [reported in Stumm and Morgan (24), Fig. 13.29, pp. 812–816] for interaction involving adsorption followed by surface precipitation via heterogeneous nucleation.

Formation of a solid phase may proceed via homogeneous nucleation (when the critical supersaturation ratio is exceeded) or at lower saturation ratio on a suitable nucleating surface, e.g., the process of heterogeneous nucleation (24). Therefore, a solid phase formed heterogeneously could have a slightly lower solubility than the homogeneous phase, especially if sufficient reaction time is not available during the latter process to attain equilibrium. However, if the Cu^{2+} ion is incorporated as a minor constituent in a solid solution (e.g., $Fe_xCu_{1-x}OOH$), Cu solubility should be significantly lower than with the pure $Cu(OH)_2$(s) phase (24, 26). With heterogeneous nucleation, the interface is fixed and there is no migration of ions across the interface (24). On the other hand, solid solution formation involves a mixing zone where the sorbate and sorbent ions are intermingled and thus susceptible to simultaneous incorporation into a single lattice. Whereas heterogeneous nucleation can reduce the extent of supersaturation necessary to initiate precipitation, solid solution formation facilitates precipitation at conditions *undersaturated* with respect to a pure phase (24). Since the surface precipitate formed during HFO–ADS was only slightly less soluble than Cu-PPT, it implies that HFO particles simply nucleate precipitation of $Cu(OH)_2$(s) and there is no solid solution formation. This assertion is supported by the XRD data provided in a later section.

HFO–CPT

The isotherms for HFO–CPT and HFO–ADS are nearly parallel over the entire log Cu_T range and the breakpoints between regions occur at similar Cu_T (Fig. 1). Such behavior has also been observed for Cr(III) adsorption and coprecipitation by HFO (4). For HFO–CPT the site densities are higher than for HFO–ADS, with the Type 1 density being 0.066 mol Cu/mol Fe ($\log \Gamma_{Cu} = -1.18$) and the Type 2 site density being equal to 0.437 ($\log \Gamma_{Cu} = -0.36$), the latter being in good agreement with the value of 0.42 observed for Cr(III) by Charlet and Manceau (4).

Using extended X-ray absorption fine structure spectroscopy (EXAFS), Charlet and Manceau (4) showed that during HFO–CPT of Cr(III) a mixed Fe–Cr oxyhydroxide ($Fe_{0.994}Cr_{0.006}OOH$) phase is formed. In contrast, Waychunas *et al.* (13) did not observe a new oxyhydroxide phase during As(V) coprecipitation with HFO despite a Γ_{As} as high as 0.7 mol As/mol Fe. This high Γ_{As} was attributed to adsorption of As(V) during the growth of HFO crystallites. During HFO–CPT, As(V) apparently adsorbs onto extremely small HFO units that are either a single Fe octahedron or a dioctahedral chain. Therefore, there is a tremendous increase in surface site availability during coprecipitation since As(V) is adsorbed during Fe–O–Fe polymerization.

The high Γ_{Cu} (0.437) of this work warrants comment. Given the measured specific surface (187 m^2/g) and Fe content (63%) of HFO, the site density corresponding to this Γ_{Cu} is 15.8 sites/nm^2. In modeling Co(II) adsorption by α-Al_2O_3, Katz and Hayes (16) found an optimal site density of only 2–3 sites/nm^2. A site density of 2.5 sites/nm^2 requires a surface area of 1182 m^2/g to yield a Γ_{Cu} of 0.437. Therefore, enhanced Cu removal during HFO–CPT was likely to be more than a simple surface area effect and could be attributed to a combination of (a) mixed (Fe, Cu) oxyhydroxide formation and (b) adsorption of Cu during the growth of HFO crystallites. As with HFO–ADS, the HFO–CPT isotherm increases sharply at log Cu_T values close to that of Cu_{sat} observed during Cu-PPT.

HAO–ADS and HAO–CPT

The HAO isotherms (Fig. 2) have similar shape to those of HFO. The linear region extends to Cu_T of $10^{-6.6}$ M (compa-

rable to HFO), whereas the upper limit of Freundlich region is reduced to a Cu_T of $10^{-5.4}$ M (an order of magnitude lower than observed for HFO). The Type 1 site densities were 0.009 mol Cu/mol Al (log $\Gamma_{Cu} = -2.05$) and 0.013 (log $\Gamma_{Cu} = -1.88$) for HAO–ADS and HAO–CPT, respectively, both lower than for HFO. The Type 2 site densities, determined from the abrupt change in slope at log $Cu_T \approx -5.4$, were 0.063 (log $\Gamma_{Cu} = -1.2$) and 0.1 (log $\Gamma_{Cu} = -1.00$) for HAO–ADS and HAO–CPT, respectively, much lower than the value expected for amorphous oxide sorbents. This could reflect incipient surface precipitation at more than an order of magnitude lower Cu_T of $10^{-5.4}$ M compared to Cu_{sat} ($10^{-3.8}$ M). The K_{spCu} of the surface precipitate formed during HAO–ADS is $10^{8.35}$ (mean $Cu_T = 10^{-5.22}$ M). Because surface precipitation occurred at lower Cu_T, the saturation region was not observed in the HAO isotherms, resulting in low Type 2 site densities.

At Γ_{Cu} below 10^{-1}, HAO–CPT appears to enhance Cu sorption compared to that seen with HAO–ADS. The magnitude of this enhancement, however, is lower than for HFO (Fig. 1). Surface precipitates formed under both adsorption and coprecipitation conditions for HAO have similar solubilities. From these experiments, a coprecipitate cannot be unambiguously distinguished from a discrete mixture of Al and Cu (hydr)oxides. However, the significant lowering of Cu solubility (1.5 orders of magnitude) associated with this surface precipitation is consistent with formation of a solid solution (i.e., mixed Al, Cu oxide). Since HFO is less soluble than HAO (from our residual Fe/Al measurements), higher aqueous Al might increase the tendency to form a solid solution. Figure 2 also indicates the Cu_{sat} for tenorite [CuO(s)] formation. The onset of surface precipitation occurs at soluble levels higher than Cu_{sat} for CuO(s) but lower than $Cu(OH)_2$(s). These results could also be explained by invoking the formation of a more crystalline Cu (hydr)oxide phase in the presence of HAO compared to the homogeneously precipitated $Cu(OH)_2$(s). However, given the relatively short reaction time, such a dramatic change in the crystallinity of Cu (hydr)oxide solid phase is less plausible than solid solution formation. The shapes of our HAO isotherms are also remarkably similar to those proposed in Van Cappellen (25) for systems where solid solution formation occurs.

Upon comparison of all the isotherms in Figs. 1 and 2, it is apparent that at $\Gamma_{Cu} < 10^{-1.2}$, Cu sorption follows the order HFO–CPT > HAO–CPT ≈ HFO–ADS > HAO–ADS. In this lower Γ_{Cu} region, corresponding to a low sorbate/sorbent ratio, Cu removal occurs solely by adsorption. Previous studies confirm that HFO is a slightly better sorbent than HAO when adsorption dominates removal (9). However, at higher sorbate/sorbent ratios, where removal is dominated by surface precipitation, HAO exhibited greater removal than HFO. Quantitatively, precipitation commences on the HAO surface when the soluble Cu is roughly 1/10th the level needed to initiate precipitation on the HFO surface.

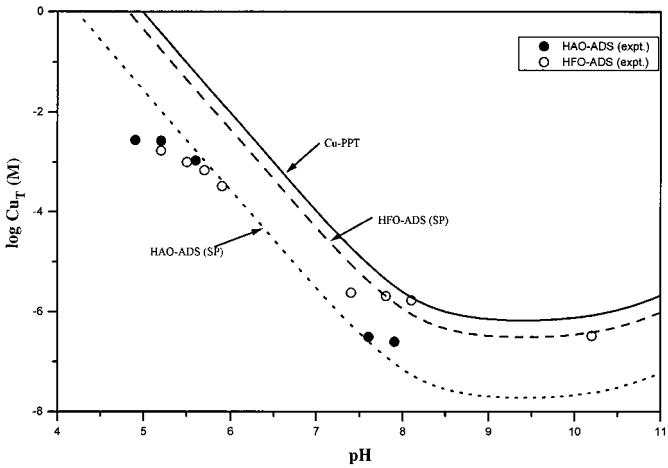

FIG. 3. Solubility of surface precipitates (SP) formed during HAO–ADS and HFO–ADS in comparison to Cu-PPT. [K_{spCu}s of the surface precipitates were obtained from the isotherms. Experimental (expt.) data plotted correspond to residual soluble Cu levels measured when obtaining solids for XRD analysis].

X-ray Diffraction Analysis

HFO–ADS. In an earlier publication (15), we investigated ADS/CPT of Cu by HFO and HAO using pH as the master variable. The surface Cu loadings, and therefore the nature of Cu interaction with the surface, will be influenced by pH. As with the sorption isotherms, in the pH-edge study we found that below pH 6.5 (low removal conditions and hence low Γ_{Cu}) HFO–ADS resulted in greater Cu uptake than HAO–ADS. However, above pH 6.5, HAO–ADS consistently produced higher Cu removal than HFO–ADS. The fact that HAO–ADS was more efficient than HFO–ADS could be attributed to the onset of surface precipitation at a lower surface coverage, hence lower pH, in the presence of HAO compared to HFO. XRD patterns for solids generated at different pH values (at constant $[Cu]_T$ loading) will be used to distinguish adsorption from surface precipitation. Specifically, the XRD data will be used to discern the nature of surface precipitation reaction, i.e., solid solution formation versus heterogeneous nucleation. It is believed (27) that simple adsorption does not alter oxide crystal dimensions, whereas solid solution formation will change lattice geometry and, in turn, XRD patterns.

Figure 3 illustrates the link between the sorption isotherm data and the pH-effect on the adsorption/surface precipitation domains. In this figure, Cu solubility limits (solid and dashed lines) of the surface precipitates formed during HAO–ADS and HFO–ADS are compared to that of Cu-PPT. These plots were constructed using the respective solubility products (K_{spCu}) of the surface precipitates obtained from the isotherms ($10^{9.46}$ for HFO–ADS; $10^{8.35}$ for HAO–ADS; $10^{9.88}$ for Cu-PPT). The data points correspond to the residual soluble Cu (Cu_T) measured when generating solids for XRD analysis. For HFO–ADS and HAO–ADS, at pH < 7.5 and < 5.6, respectively, the Cu_T values are lower than the levels dictated by the solubility of the surface precipitate.

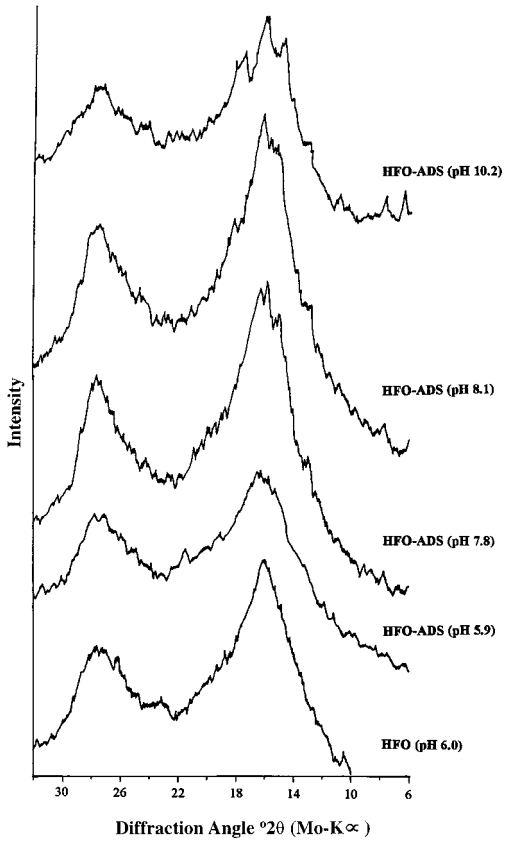

FIG. 4. X-ray diffraction patterns of HFO–ADS samples.

Therefore, under the experimental conditions used to generate the XRD samples, surface precipitation is expected above pH 7.5 and 5.6, respectively, for HFO–ADS and HAO–ADS. Comparing XRD patterns above and below these pH values can provide insight into the type of interaction between Cu and the hydrous oxides. Also, for Cu_T of $10^{-2.47}$ M used in the XRD experiments, homogeneous Cu precipitation (Cu-PPT) can be expected at pH 6.22 (based on Fig. 3).

Patterns for pure HFO and with Cu adsorbed at different pH values are shown in Fig. 4. The XRD pattern for the pure HFO at pH 6.0 is characteristic of a 2-line ferrihydrite (28) and, though not shown, is similar to patterns for pure HFO at pH 7.8 and 10.4. With Cu adsorbed at pH 5.9, the pattern resembles pure HFO but with greater disorder as indicated by shorter peak heights. There are no peaks characteristic of hydrous Cu oxide (HCO), suggesting no surface precipitation. The diffraction pattern obtained for HCO formed under Cu-PPT conditions exhibited peaks at 14.9°, 16.2°, 17.6°, 22°, 25.95°, 27.3°, 29.2°, and 29.9° 2θ characteristic of CuO(s) and at 7.6°, 11.1°, 24.1°, and 28° 2θ attributable to $Cu(OH)_2$(s) (21, 22).

XRD patterns for the samples at pH 7.8, 8.1, and 10.2 show new peaks not observed for the pH 5.9 sample. These samples also have the characteristic 2-line ferrihydrite peaks. With increasing pH, secondary peaks can be observed as shoulders around the main ferrihydrite peak at of 16° 2θ. For the sample at pH 10.2 the peaks at 7.6°, 10.8°, 14.9°, 17.6°, 18.2°, and 24.1° 2θ likely result from CuO(s) or $Cu(OH)_2$(s), although not all their characteristic peaks are observed. These patterns suggest the presence of HCO in the sample precipitated either homogeneously or present on the HFO surface above pH 7.8. It is essential to note from Fig. 4 that patterns corresponding to surface Cu precipitation are observable only at pH values greater than that corresponding to bulk precipitation of Cu. Harvey and Linton (8) also found, using X-ray photoelectron spectroscopy, that surface precipitation of Cu on HFO occurs only when bulk homogeneous precipitation of $Cu(OH)_2$(s) is favored.

HFO–CPT. Diffraction patterns were obtained for samples at three different pH values under CPT conditions (Fig. 5). The pH 5.8 sample pattern resembles pure HFO. However, in contrast to HFO–ADS, the patterns for samples at higher pH (8.2 and 10.4) have no peaks characteristic of HCO (secondary peaks surrounding the main ferrihydrite peak at 16° 2θ), indicating the absence of surface Cu precipitation. It was difficult to match patterns for HFO–CPT with those of a mixed (Fe, Cu) oxide like copper-spinel [$CuFe_2O_4$(s)]. This spinel has major peaks around 16° and 27.5° 2θ, which would be masked by the major peaks for HFO. Therefore, unlike HAO–CPT discussed below, XRD could not resolve whether mixed oxide formation or adsorption on HFO crystallites was the predominant mechanism for HFO–CPT.

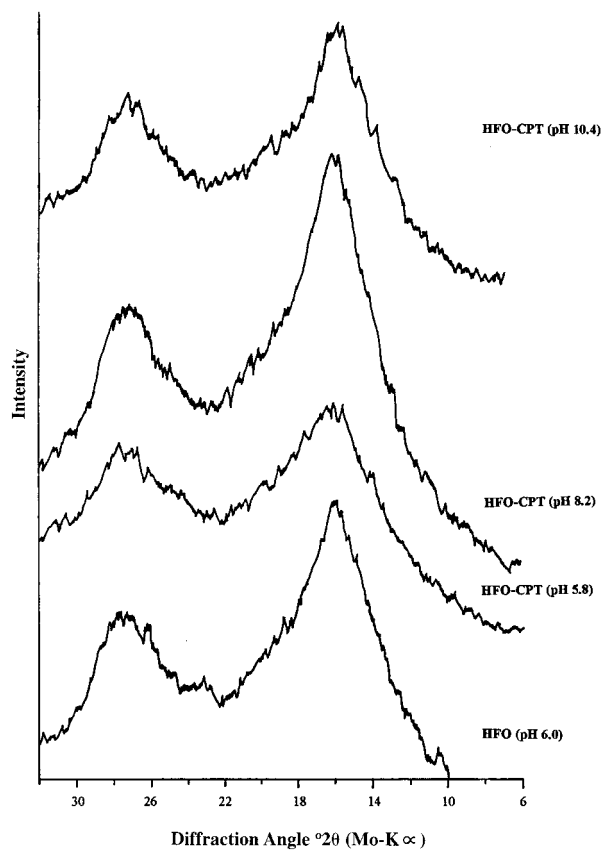

FIG. 5. X-ray diffraction patterns of HFO–CPT samples.

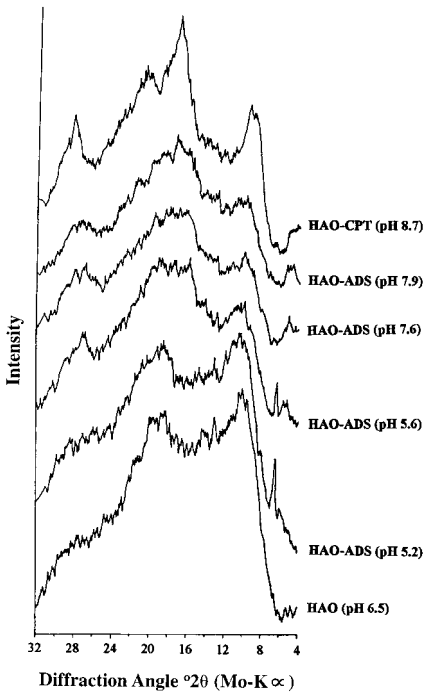

FIG. 6. X-ray diffraction patterns of HAO–ADS samples.

HAO–ADS. The diffraction patterns for HAO–ADS are shown in Fig. 6. The pattern at pH 5.2 and pH 4.9 (not shown) resembles that of HAO at pH 6.5 [XRD patterns for HAO obtained up to pH < 9 (not shown) are also similar to those of the pH 6.5 sample]. Diffraction patterns start to deviate from that of pure HAO at pH > 5.6, but peaks characteristic of $Cu(OH)_2$(s) and CuO(s) are not observed. Therefore, from Fig. 6 one can surmise that during HAO–ADS, adsorption appears to be the dominant reaction below pH 5.6, above which surface precipitation of a solid solution dominates removal. Also, the patterns for HAO–ADS at pH above 5.5 are similar to those of HAO–CPT (Fig. 6 [topmost pattern] and Fig. 7). In contrast to HFO–ADS, patterns indicative of surface Cu precipitation are evident during HAO–ADS at pH 5.6. This pH value is lower than that required for homogeneous precipitation.

Surface coverage for the different HAO–ADS samples was calculated assuming the 0.25 mol Cu adsorption sites/mole Al obtained from our HFO–ADS isotherm. Under HAO–ADS conditions, 8.7×10^{20} total sites are available for Cu adsorption. Based on Cu removal at pH 5.6 and 5.2, about 61.4 and 21.2%, respectively, of the total HAO surface sites are occupied by Cu.

The surface coverage at pH 5.6 is sufficient to induce surface precipitation. Xia *et al.* (14), using EXAFS, showed that Cu(II) hydroxide clusters form on silica surfaces even at surface loadings as low as 0.8% of a monolayer coverage. Charlet and Manceau (4) present evidence for multinuclear Cr(III) complex formation on HFO at surface coverage of 10%. Similarly, other EXAFS studies indicate the formation of Co(II), Cr(III), and Ni(II) polynuclear species at surface coverages as low as 5% of a monolayer coverage (29–32). Besides possessing high surface coverage, the reaction time in our study (45 min) was also adequate for surface precipitation. Scheidegger *et al.* (32) found that during Ni(II) sorption on pyrophyllite, surface precipitates were observed after about 15 min reaction time.

The XRD pattern for HFO–ADS at pH 5.9 (Fig. 4) does not indicate surface precipitate formation, although XRD is less sensitive than EXAFS. Based on surface coverage calculations, about 68% of the total sorption sites were occupied by Cu at pH 5.9. With HFO–ADS, XRD patterns begin to show evidence of precipitate formation (pH 7.8) when the surface coverage is about 75%. It thus appears that surface precipitation occurs at a lower pH and coverage during adsorption onto HAO than that onto HFO. XRD seems to provide a simple and convenient tool in this case for distinguishing surface adsorption from a precipitation reaction.

HAO–CPT. The diffraction tracings for HAO–CPT (Fig. 7) differ markedly from that of pure HAO. At pH 8.7, the peak positions at 16.8°, 20.4°, and 28.4° 2θ can be attributed to a mixed (Al, Cu) oxide—$CuAl_2O_4$(s) (22) [a peak at 14.27° 2θ for $CuAl_2O_4$(s) was not observed]. The relative peak intensities also match well with those for $CuAl_2O_4$(s). Based on the evidence, we conclude that a mixed (Al, Cu) oxide forms during HAO–CPT.

Since the diffraction patterns are similar for HAO–ADS (above pH 5.6) and HAO–CPT, it suggests that surface precipitation under HAO–ADS conditions also resulted in the formation of a mixed oxide. Mixed metal oxides typically have lower solubilities than their pure counterparts (26). Our mac-

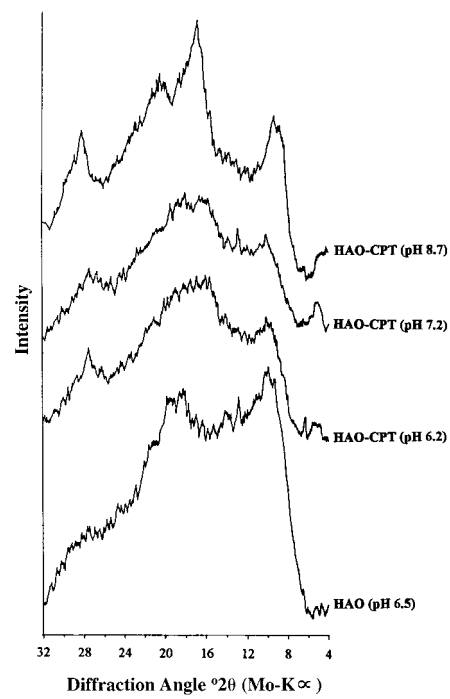

FIG. 7. X-ray diffraction patterns of HAO–CPT samples.

roscopic studies also indicated that the solubility of HAO surface Cu precipitate is lower than that for its HFO analog. The differences in solubility are attributable to the differences in the nature of the surface Cu precipitate. During HFO–ADS surface precipitation likely forms a discrete mixture of HFO and HCO, whereas under HAO–ADS a mixed (Al, Cu) oxide is formed. Although compelling evidence to support this hypothesis is provided, use of an *in situ* spectroscopic technique like EXAFS would further elucidate the coordinative environments that exist during adsorption and coprecipitation.

CONCLUSIONS

Cu removal from aqueous solutions at circumneutral pH was markedly influenced by the sorbate/sorbent ratio and contact methodology. Under both ADS and CPT, higher Cu sorption was observed with HFO than HAO at low sorbate/sorbent ratio. This confirmed the generally held notion that HFO is more reactive in binding heavy metal cations than HAO. At these low ratios, more Cu was retained after CPT than after ADS for both oxides.

At high surface coverage with elevated sorbate/sorbent ratios, more complicated behavior is observed because surface precipitation becomes a dominant contributor to the overall "apparent" sorption. Compared to HFO, surface precipitation (for both ADS and CPT) occurred at a lower pH and surface coverage in the presence of HAO. Thus, for a grossly Cu-contaminated waste source, on an equimolar basis, HAO might be a superior sorbent to HFO. An extremely high sorption density (0.437 mol Cu/mol Fe) was observed for HFO–CPT, indicating either mixed oxide formation or continual replenishment of Cu-sorbing sites at the surface of growing HFO crystallites. In a practical sense, this higher site density with HFO–CPT means a lower coagulant dosage for water/wastewater treatment compared to that required for HFO–ADS.

XRD patterns suggest that surface precipitation during HFO–ADS results in a discrete mixture of HFO and HCO. For HAO–ADS, XRD patterns reveal the formation of surface precipitate at lower pH and surface coverage than that required during HFO–ADS, validating our macroscopic observations. In addition, the surface precipitate formed during HAO–ADS is similar to that of the species formed during HAO–CPT, which resembles that of a mixed (Al, Cu) oxide ($CuAl_2O_4$) (s). Existence of such an oxide during HAO–ADS implies a surface precipitate with lower solubility than that formed during HFO–ADS.

ACKNOWLEDGMENT

The authors thank Dr. Earle R. Ryba, Associate Professor of Metallurgy, The Pennsylvania State University (University Park, PA), for his valuable assistance in XRD data collection and analysis.

REFERENCES

1. Lutzenkirchen, J., and Behra, Ph., *Aqua. Geochem.* **1,** 375 (1996).
2. Xu, Y., Schwartz, F. W., and Traina, S. J., *Environ. Sci. Technol.* **28,** 1472 (1994).
3. Benjamin, M. M., and Leckie, J. O., *J. Colloid Interface Sci.* **79,** 209 (1981).
4. Charlet, L., and Manceau, A., *J. Colloid Interface Sci.* **148,** 443 (1992).
5. Crawford, R. J., Harding, I. H., and Mainwaring, D. E., *Langmuir* **9,** 3050 (1993).
6. Dzombak, D. A., and Morel, F. M. M., *J. Colloid Interface Sci.* **112,** 588 (1986).
7. Farley, K. J., Dzombak, D. A., and Morel, F. M. M., *J. Colloid Interface Sci.* **106,** 226 (1985).
8. Harvey, D. T., and Linton, R. W., *Colloids Surf.* **11,** 81 (1984).
9. Kinniburgh, D. G., Jackson, M. L., and Syers, J. K., *Soil Sci. Soc. Am. J.* **40,** 796 (1976).
10. McBride, M. B., *Soil Sci. Soc. Am. J.* **42,** 27 (1978).
11. Spadini, L., Manceau, A., Schindler, P. W., and Charlet, L., *J. Colloid Interface Sci.* **168** (1994).
12. Swallow, K. C., Hume, D. N., and Morel, F. M. M., *Environ. Sci. Technol.* **14,** 1326 (1980).
13. Waychunas, G. A., Rea, B. A., Fuller, C. C., and Davis, J. A., *Geochim. Cosmochim. Acta* **57,** 2251 (1993).
14. Xia, K., Mehadi, A., Taylor, R. W., and Bleam, W. F., *J. Colloid Interface Sci.* **185,** 252 (1997).
15. Karthikeyan, K. G., Elliott, H. A., and Cannon, F. S., *Environ. Sci. Technol.* **31,** 2721 (1997).
16. Katz, L. E., and Hayes, K. F., *J. Colloid Interface Sci.* **170,** 477 (1995).
17. Katz, L. E., and Hayes, K. F., *J. Colloid Interface Sci.* **170,** 491 (1995).
18. Baltpurvins, K. A., Burns, R. C., and Lawrance, G. A., *Environ. Sci. Technol.* **30,** 939 (1996).
19. De Hek, H., Stol, R. J., and De Bruyn, P. L., *J. Colloid Interface Sci.* **64,** 73 (1978).
20. Violante, A., and Huang, P. M., *Clays Clay Miner.* **33,** 181 (1985).
21. Karthikeyan, K. G., "Adsorption and Coprecipitation of Copper by the Hydrous Oxides of Iron and Aluminum: Macroscopic, Modeling, and Spectroscopic Analysis," Ph.D. Dissertation. The Pennsylvania State University, University Park, PA, 1997.
22. JCPDS, "Powder Diffraction File: Inorganic Phases." International Centre for Diffraction Data, Swarthmore, PA, 1989.
23. Dzombak, D. A., and Morel, F. M. M., "Surface Complexation Modeling." Wiley & Sons, New York, 1990.
24. Stumm, W., and Morgan, J. J., "Aquatic Chemistry: Chemical Equilibria and Rates in Natural Waters." Wiley & Sons, New York, 1996.
25. Van Cappellen, "The Formation of Marine Apatite; A Kinetic Study," Ph.D. Thesis. Yale University, New Haven, CT, 1991.
26. McBride, M. B., "Environmental Chemistry of Soils." Oxford Univ. Press, New York, 1994.
27. Stumm, W., and Morgan, J. J., "Aquatic Chemistry." Wiley–Interscience, New York, 1970.
28. Schwertzmann, U., and Cornell, R. M., "Iron Oxides in the Laboratory, Preparation and Characterization." Weinheim, New York, 1991.
29. Fendorf, S. E., Lamble, G. M., Stapleton, M. G., Kelley, M. J., and Sparks, D. L., *Environ. Sci. Technol.* **28,** 284 (1994).
30. Fendorf, S. E., and Sparks, D. L., *Environ. Sci. Technol.* **28,** 290 (1994).
31. O'Day, P. A., Parks, G. A., and Brown, G. E., Jr., *Clays Clay Miner.* **42,** 337 (1994).
32. Scheidegger, A. M., Lamble, G. M., and Sparks, D. L., *Environ. Sci. Technol.* **30,** 548 (1996).